Active and Passive Beamforming for IRS-Aided Vehicle Communication

Xiangping Kong[1], Yu Wang[1,2*], Lei Zhang[1], Yulong Shang[1] and Ziyan Jia[1]
[1] School of Electrical and Information Engineering, Jiangsu University of Technology
Changzhou, Jiangsu 213001 China
[2] National Mobile Communications Research Laboratory, Southeast University
Nanjing, Jiangsu 210096 China
[e-mail: yuwang_edina@jsut.edu.cn]
[*]Corresponding author: Yu Wang

Received October 9, 2022; revised March 28, 2023; accepted April 24, 2023; published May 31, 2023

Abstract

This paper considers the jointly active and passive beamforming design in the IRS-aided MISO downlink vehicle communication system where both V2I and V2V communication paradigms coexist. We formulate the problem as an optimization problem aiming to minimize the total transmit power of the base station subject to SINR requirements of both V2I and V2V users, total transmit power of base station and IRS's phase shift constraints. To deal with this non-convex problem, we propose a method which can alternately optimize the active beamforming at the base station and the passive beamforming at the IRS. By using first-order Taylor expansion, matrix analysis theory and penalized convex-concave process method, the non-convex optimization problem with coupled variables is converted into two decoupled convex sub-problems. The simulation results show that the proposed alternate optimization algorithm can significantly decrease the total transmit power of the vehicle base station.

Keywords: Intelligent reflecting surface, convex optimization, vehicular communication, V2I and V2V communication, beamforming.

This work is supported by National Natural Science Foundation of China (No. 61901196, 61701202), the open research fund of National Mobile Communications Research Laboratory, Southeast University (No. 2021D14), Future Network Scientific Research Fund Project (No. FNSRFP-2021 -YB-35), Changzhou Sci&Tech Program (No. CJ20210070), Changzhou Key Laboratory of 5G + Industrial Internet Fusion Application (No. CM20223015)

http://doi.org/10.3837/tiis.2023.05.011 **ISSN : 1976-7277**

1. Introduction

With the development of transportation system and mobile network communication, the related research on vehicle communication technology for the internet of vehicles (IoV) is also increasing. The IoV can provide convenient life style to human. However, the wireless communication in IoV is easily affected by several factors [1]. For example, the occlusion of buildings will lead to the deterioration of the propagation link of vehicle communication. Intelligent reflecting surface (IRS) is presented to assist the wireless communication of vehicles [2]. By intelligently controlling the reflective phases, IRS can adaptively change the transmission environment so as to improve system spectral efficiency and network coverage. Therefore, the IRS-assisted vehicle communication problems have received extensive attentions. The authors of [3] have enhanced the property of vehicle-to-infrastructure (V2I) communication systems by optimizing the beamforming of IRS and base station (BS), and also propounded a new reinforcement learning algorithm that is based on deep deterministic policy gradient (DDPG). The authors of [4] have studied a millimeter wave vehicle communication system to maximize the rate of the uplink with the assistance of IRS, and designed a scheme to reduce the channel estimation overhead associated with using IRS. As the radio wave will encounter many objects in the propagation process that can lead to transmission distortion in the vehicular environment, the maximization of the minimum average bit rate is finally achieved by optimizing the beamforming of the IRS and the resource allocation of the road side unit (RSU) in [5]. The authors of [6] have studied the use of hybrid orthgonal multiple access/non-orthgonal multiple access (OMA/NOMA)-enabled access schemes in highly dynamic environments. However, the above studies have not considered the case of V2I and vehicle-to-vehicle (V2V) links both of which share the same spectrum.

In this paper, we investigate the performance improvement brought by deploying an IRS in the MISO downlink IoV system to assist V2I and V2V communications. The beamforming design problem is formed to minimize the BS transmit power subject to SINR requirements of V2I and V2V users, total transmit power and IRS phase shift constraints. There is a strong coupling relationship between the beamforming vector at the BS and the phase shift matrix of the IRS. By using the first-order Taylor expansion method and matrix analysis theory, we convert the non-convex optimization problem with coupled variables into two decoupled convex sub-problems. Then the CVX solver is used to solve the convex problems. Finally, simulation results proved the convergence of the algorithm and verified the superiority of the proposed approach compared with other benchmarks. We showed the effect of the number of IRS elements and the deployment location on the BS transmit power. The total minimum transmit power can be reduced when increasing the number of IRS elements. Moreover, the transmit power of the BS decreases with the decrease of the distance between the BS and the IRS.

The remainder of this paper is organized as follows. Section II describes the system model in this paper. Section III shows the specific processing of beamforming design. Section IV shows the results of simulations performed on the system. Section V concludes this paper.

2. System Model

Fig. 1 shows the IRS-assisted downlink IoV scenario considered in this paper. IRS is deployed on the roadside to assist IoV communication, and the coverage scope of the cellular BS includes a cellular-vehicle user equipment (C-VUE) and a pair of device-to-device-vehicle user equipment (D-VUE) where D-VUE1 is transmitter, and D-VUE2 is receiver. The channel from BS to C-VUE is regarded as a V2I link and the channel from D-VUE1 to D-VUE2 is regarded as a V2V link. Considering the MISO system, the antennas numbers of BS and D-VUE1 are M_t and L_t, respectively. The antennas number of C-VUE and D-VUE2 is 1, the number of reflective cells in IRS is N. The C-VUE and D-VUE2 receive their incident signals from the BS and the D-VUE1, respectively. In order to improve spectrum utilization of the IoV, V2V link and V2I link is designed to work on the same spectrum resource. Thereby the C-VUE and the D-VUE2 will be interfered by each other. The IRS deployed at the roadside can help to alleviate this problem and enhanced the desired link signal without additional power consumption and deployment costs. To this end, the total transmit power of the BS is minimized by jointly optimizing the (active) transmit beamforming of the BS and the (passive) reflection beamforming of the IRS phase shifter.

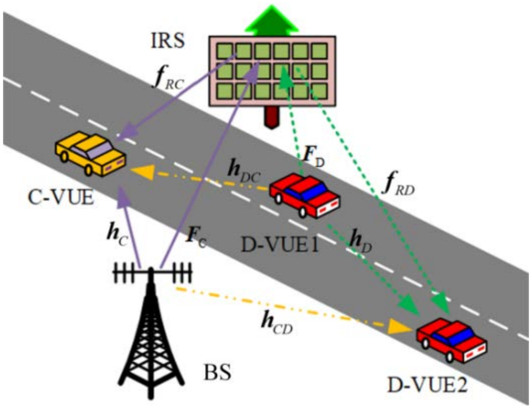

Fig. 1. IRS-assisted IoV communication scenario

2.1 Channel Model

For V2I user, the BS sends the signal to C-VUE, and for V2V user, D-VUE1 vehicle sends the signal to D-VUE2. Due to the assistance and beam steering of the IRS, the downlink signals from the BS and D-VUE1 will be reflected to the C-VUE and D-VUE2 through the IRS, respectively. Thus, the received signals from C-VUE and D-VUE2 are the superposition of two-way signals, one from the direct path and the other from the indirect path through the IRS[7]. Since V2I users and V2V users share spectrum, C-VUE will experience interference from D-VUE1, and similarly, D-VUE2 will experience interference from cellular BS. **Fig. 1** illustrates channel descriptions. The channels among the BS and IRS, D-VUE1 and IRS, IRS and C-VUE, IRS and D-VUE2 are denoted as $\boldsymbol{F}_C \in \mathbb{C}^{N\times M_t}$, $\boldsymbol{F}_D \in \mathbb{C}^{N\times L_t}$, $\boldsymbol{f}_{RC} \in \mathbb{C}^{N\times 1}$, $\boldsymbol{f}_{RD} \in \mathbb{C}^{N\times 1}$, respectively. The direct channels among the BS and C-VUE, the D-VUE1 and D-VUE2, the BS and D-VUE2, the D-VUE1 and C-VUE are denoted as $\boldsymbol{h}_C \in \mathbb{C}^{M_t\times 1}$, $\boldsymbol{h}_D \in \mathbb{C}^{L_t\times 1}$, $\boldsymbol{h}_{CD} \in \mathbb{C}^{M_t\times 1}$, $\boldsymbol{h}_{DC} \in \mathbb{C}^{L_t\times 1}$, respectively.

The phase shifts of the reflective element (with an amplitude of 1) in the IRS can be adjusted according to specific needs and thus used to strengthen the user incident signal and inhibit interference. $\boldsymbol{\Phi} = \mathrm{diag}\{\phi_1, \phi_2, ..., \phi_N\}$ delegate to the phase shift matrix of the IRS, $\phi_n = e^{j\theta_n}$ delegates the reflection element with a phase shift of $\theta_n \in [0, 2\pi]$, $n = 1, 2, ..., N$. Since the IRS has the ability to control the beam direction, it can be hypothesized that the communication channel among the BS and the IRS, and the channels among the IRS and the vehicle terminals are Rice channels. The rest of the channels are Rayleigh channels [8]. The Rice channel can be modeled as

$$F_x = \sqrt{\rho d_x^{-\alpha_x}} \left(\sqrt{\frac{\kappa_x}{1+\kappa_x}} F_x^{LoS} + \sqrt{\frac{1}{1+\kappa_x}} F_x^{NLoS} \right), \mathrm{x} \in \{\mathrm{C}, \mathrm{D}, \mathrm{RC}, \mathrm{RD}\}, \tag{1}$$

where d_x is the distance between the transceiver of the link x, α_x is the path loss index. ρ is the path loss at a reference range of 1m, κ_x is the Rice fading factor, F_x^{NLoS} is the non-line-of-sight random scattering path of the link x, which can be described by a standard complex Gaussian distribution. F_x^{LoS} is the line of sight , which can be characterized by the antenna array response at both the transceiver and the IRS. Assuming that the antennas at the transceiver and the IRS are arranged in a uniform linear array (ULA) [9], the antenna array response containing m elements can be modeled as

$$a_m(\varphi) = \left[1, e^{j2\pi \frac{d}{\lambda}\sin\varphi}, ..., e^{j2\pi \frac{d}{\lambda}(m-1)\sin\varphi}\right], \tag{2}$$

where λ is electromagnetic wave wavelength, φ is the beam angle of arrival (AoA) or beam angle of departure (AoD) of a single array element/antenna [10]. Hence, the line-of-sight link can be denoted as

$$F_x^{LoS} = a_{|x_1|}^{\mathrm{H}}(\varphi_{\mathrm{AoA,x}}) a_{|x_2|}(\varphi_{\mathrm{AoD,x}}) , \mathrm{x} \in \{\mathrm{C}, \mathrm{D}, \mathrm{RC}, \mathrm{RD}\}, \tag{3}$$

where $\varphi_{\mathrm{AoA,x}}$ is the AoA at the receiver antenna of link x, $\varphi_{\mathrm{AoD,x}}$ is the AoD at the transmitter antenna of link x, and $|x_1|$ and $|x_2|$ are the figures of array elements/antennas at the receiver and transmitter, respectively.

The Rayleigh channel can be expressed as

$$h_x = \sqrt{\rho d_x^{-\alpha_x}} \tilde{h}_x, \mathrm{x} \in \{\mathrm{C}, \mathrm{D}, \mathrm{DC}, \mathrm{CD}\}, \tag{4}$$

where $\tilde{h}_x$ is a random scattering path, which can be characterized by an independent complex Gaussian distribution.

2.2 SINR Analysis

The transmitted signals of the BS and D-VUE1 are $x_C = w s_C$ and $x_D = w_D s_D$, respectively, where $w \in \mathbb{C}^{M_t \times 1}$ and $w_D \in \mathbb{C}^{L_t \times 1}$ are the transmission precoding vector of the BS and D-VUE1, respectively. $s_C \in \mathbb{C}$ and $s_D \in \mathbb{C}$ are the orthogonal symbol vectors sent by the C-VUE and D-VUE, respectively [11], satisfying $\mathbb{E}[s_C s_C^*] = 1$, $\mathbb{E}[s_D s_D^*] = 1$, and $\mathbb{E}[s_C s_D^*] = 0$.

The received signals of C-VUE and D-VUE are

$$y_C = (h_C^H + f_{RC}^H \Phi F_C) w s_C + (h_{DC}^H + f_{RC}^H \Phi F_D) w_D s_D + n_C, \tag{5}$$

$$y_D = (h_D^H + f_{RD}^H \Phi F_D) w_D s_D + (h_{CD}^H + f_{RD}^H \Phi F_C) w s_C + n_D, \tag{6}$$

where $n_C \sim CN(0, \sigma_C^2)$, $n_D \sim CN(0, \sigma_D^2)$ are complex Gaussian white noise.

The received signal to interference plus noise ratio (SINR) of C-VUE and D-VUE are

$$SINR_C = \frac{\left|(h_C^H + f_{RC}^H \Phi F_C) w\right|^2}{\left|(h_{DC}^H + f_{RC}^H \Phi F_D) w_D\right|^2 + \sigma_C^2}, \tag{7}$$

$$SINR_D = \frac{\left|(h_D^H + f_{RD}^H \Phi F_D) w_D\right|^2}{\left|(h_{CD}^H + f_{RD}^H \Phi F_C) w\right|^2 + \sigma_D^2}. \tag{8}$$

The transmit precoding vector at the D-VUE1 adopts an ideal form, that is, w_D is defined as the right singular vector corresponding to the largest singular value of the channel gain matrix by using singular value decomposition (SVD) [12].

3. Beamforming Design

By optimizing the beamforming vector $\boldsymbol{w}$ at the BS and the phase shift matrix $\boldsymbol{\Phi}$ at the IRS, the transmit power of the BS can be minimized as P1. P1 shows the overall optimization problem.

$$\text{P1}: \quad \min_{\boldsymbol{w},\boldsymbol{\Phi}} \|\boldsymbol{w}\|^2, \tag{9}$$

$$s.t. \quad \frac{|(\boldsymbol{h}_C^H + \boldsymbol{f}_{RC}^H\boldsymbol{\Phi}\boldsymbol{F}_C)\boldsymbol{w}|^2}{|(\boldsymbol{h}_{DC}^H + \boldsymbol{f}_{RC}^H\boldsymbol{\Phi}\boldsymbol{F}_D)\boldsymbol{w}_D|^2 + \sigma_C^2} \geq \gamma_1, \tag{9a}$$

$$\frac{|(\boldsymbol{h}_D^H + \boldsymbol{f}_{RD}^H\boldsymbol{\Phi}\boldsymbol{F}_D)\boldsymbol{w}_D|^2}{|(\boldsymbol{h}_{CD}^H + \boldsymbol{f}_{RD}^H\boldsymbol{\Phi}\boldsymbol{F}_C)\boldsymbol{w}|^2 + \sigma_D^2} \geq \gamma_2, \tag{9b}$$

$$\|\boldsymbol{w}\|^2 \leq P, \tag{9c}$$

$$|[\boldsymbol{\Phi}]_{n,n}| = 1, \ n=1,2,\dots,N. \tag{9d}$$

In P1, there is a strong coupling relationship between the variables $\boldsymbol{w}$ and $\boldsymbol{\Phi}$, an alternate optimization method can be used to solve it [13]. Firstly, fix $\boldsymbol{\Phi}$ of the IRS to find the optimal solution $\boldsymbol{w}$, and then fix $\boldsymbol{w}$ to obtain the optimal $\boldsymbol{\Phi}$.

3.1 Optimize $\boldsymbol{w}$ by fixing $\boldsymbol{\Phi}$.

After moving the denominator to the right, constraint (9a) will has the following inequality

$$|(\boldsymbol{h}_C^H + \boldsymbol{f}_{RC}^H\boldsymbol{\Phi}\boldsymbol{F}_C)\boldsymbol{w}|^2 \geq (|(\boldsymbol{h}_{DC}^H + \boldsymbol{f}_{RC}^H\boldsymbol{\Phi}\boldsymbol{F}_D)\boldsymbol{w}_D|^2 + \sigma_C^2)\gamma_1. \tag{10}$$

We can reformulate $|(\boldsymbol{h}_C^H + \boldsymbol{f}_{RC}^H\boldsymbol{\Phi}\boldsymbol{F}_C)\boldsymbol{w}|^2$ as

$|(\boldsymbol{h}_C^H + \boldsymbol{f}_{RC}^H\boldsymbol{\Phi}\boldsymbol{F}_C)\boldsymbol{w}|^2 = \boldsymbol{w}^H(\boldsymbol{h}_C + \boldsymbol{F}_C^H\boldsymbol{\Phi}^H\boldsymbol{f}_{RC})(\boldsymbol{h}_C^H + \boldsymbol{f}_{RC}^H\boldsymbol{\Phi}\boldsymbol{F}_C)\boldsymbol{w}$. Formula (10) is non-convex. By exercising the first-order Taylor expansion [14], $\boldsymbol{w}^H(\boldsymbol{h}_C + \boldsymbol{F}_C^H\boldsymbol{\Phi}^H\boldsymbol{f}_{RC})(\boldsymbol{h}_C^H + \boldsymbol{f}_{RC}^H\boldsymbol{\Phi}\boldsymbol{F}_C)\boldsymbol{w}$ be lower bounded linearly by

$$2\,\text{Re}\left\{\boldsymbol{w}^{(t)^H}(\boldsymbol{h}_C + \boldsymbol{F}_C^H\boldsymbol{\Phi}^H\boldsymbol{f}_{RC})(\boldsymbol{h}_C^H + \boldsymbol{f}_{RC}^H\boldsymbol{\Phi}\boldsymbol{F}_C)\boldsymbol{w}\right\} - \boldsymbol{w}^{(t)^H}(\boldsymbol{h}_C + \boldsymbol{F}_C^H\boldsymbol{\Phi}^H\boldsymbol{f}_{RC})(\boldsymbol{h}_C^H + \boldsymbol{f}_{RC}^H\boldsymbol{\Phi}\boldsymbol{F}_C)\boldsymbol{w}^{(t)},$$

where $\boldsymbol{w}^{(t)}$ is the optimal solution at the t-th iteration. Then construct new constraints of (9a) as

$$\begin{aligned}&2\,\text{Re}\left\{\boldsymbol{w}^{(t)^H}(\boldsymbol{h}_C + \boldsymbol{F}_C^H\boldsymbol{\Phi}^H\boldsymbol{f}_{RC})(\boldsymbol{h}_C^H + \boldsymbol{f}_{RC}^H\boldsymbol{\Phi}\boldsymbol{F}_C)\boldsymbol{w}\right\} - \boldsymbol{w}^{(t)^H}(\boldsymbol{h}_C + \boldsymbol{F}_C^H\boldsymbol{\Phi}^H\boldsymbol{f}_{RC})(\boldsymbol{h}_C^H + \boldsymbol{f}_{RC}^H\boldsymbol{\Phi}\boldsymbol{F}_C)\boldsymbol{w}^{(t)}\\ &\geq (|(\boldsymbol{h}_{DC}^H + \boldsymbol{f}_{RC}^H\boldsymbol{\Phi}\boldsymbol{F}_D)\boldsymbol{w}_D|^2 + \sigma_C^2)\gamma_1\end{aligned} \tag{11}$$

The optimization problem is transformed into P2.

$$\text{P2}: \quad \min_{\boldsymbol{w}} \|\boldsymbol{w}\|^2, \tag{12}$$

$$\begin{aligned}s.t. \ &2\,\text{Re}\left\{\boldsymbol{w}^{(t)^H}(\boldsymbol{h}_C + \boldsymbol{F}_C^H\boldsymbol{\Phi}^H\boldsymbol{f}_{RC})(\boldsymbol{h}_C^H + \boldsymbol{f}_{RC}^H\boldsymbol{\Phi}\boldsymbol{F}_C)\boldsymbol{w}\right\}\\ &-\boldsymbol{w}^{(t)^H}(\boldsymbol{h}_C + \boldsymbol{F}_C^H\boldsymbol{\Phi}^H\boldsymbol{f}_{RC})(\boldsymbol{h}_C^H + \boldsymbol{f}_{RC}^H\boldsymbol{\Phi}\boldsymbol{F}_C)\boldsymbol{w}^{(t)}\\ &\geq (|(\boldsymbol{h}_{DC}^H + \boldsymbol{f}_{RC}^H\boldsymbol{\Phi}\boldsymbol{F}_D)\boldsymbol{w}_D|^2 + \sigma_C^2)\gamma_1\end{aligned}, \tag{12a}$$

$$|(\boldsymbol{h}_D^H + \boldsymbol{f}_{RD}^H\boldsymbol{\Phi}\boldsymbol{F}_D)\boldsymbol{w}_D|^2 \geq (|(\boldsymbol{h}_{CD}^H + \boldsymbol{f}_{RD}^H\boldsymbol{\Phi}\boldsymbol{F}_C)\boldsymbol{w}|^2 + \sigma_D^2)\gamma_2, \tag{12b}$$

$$\|\boldsymbol{w}\|^2 \le P \,. \tag{12c}$$

The constraints in P2 are convex constraints, so we can use CVX solver to solve it.

3.2 Optimize $\boldsymbol{\Phi}$ by fixing $\boldsymbol{w}$.

The problem to find $\boldsymbol{\Phi}$ by fixing $\boldsymbol{w}$ is a feasibility checking problem, which can be described by P3.

$$\text{P3:} \quad \text{find } \boldsymbol{\Phi}, \tag{13}$$

$$s.t. \quad \frac{\left|(\boldsymbol{h}_C^H + \boldsymbol{f}_{RC}^H \boldsymbol{\Phi} \boldsymbol{F}_C)\boldsymbol{w}\right|^2}{\left|(\boldsymbol{h}_{DC}^H + \boldsymbol{f}_{RC}^H \boldsymbol{\Phi} \boldsymbol{F}_D)\boldsymbol{w}_D\right|^2 + \sigma_C^2} \ge \gamma_1 \,, \tag{13a}$$

$$\frac{\left|(\boldsymbol{h}_D^H + \boldsymbol{f}_{RD}^H \boldsymbol{\Phi} \boldsymbol{F}_D)\boldsymbol{w}_D\right|^2}{\left|(\boldsymbol{h}_{CD}^H + \boldsymbol{f}_{RD}^H \boldsymbol{\Phi} \boldsymbol{F}_C)\boldsymbol{w}\right|^2 + \sigma_D^2} \ge \gamma_2 \,, \tag{13b}$$

$$\left|[\boldsymbol{\Phi}]_{n,n}\right| = 1, \; n=1,2,\ldots,N \,. \tag{13c}$$

Constraints (13a), (13b) and (13c) are non-convex constraints, which need to be converted into convex constraints.

Firstly, the left side of the inequality of constraint (13a) can be equivalent to

$$\frac{\left|(\boldsymbol{h}_C^H + \boldsymbol{f}_{RC}^H \boldsymbol{\Phi} \boldsymbol{F}_C)\boldsymbol{w}\right|^2}{\left|(\boldsymbol{h}_{DC}^H + \boldsymbol{f}_{RC}^H \boldsymbol{\Phi} \boldsymbol{F}_D)\boldsymbol{w}_D\right|^2 + \sigma_C^2} = \frac{\left|(\boldsymbol{h}_C^H + \boldsymbol{\phi}^H diag(\boldsymbol{f}_{RC}^H)\boldsymbol{F}_C)\boldsymbol{w}\right|^2}{\left|(\boldsymbol{h}_{DC}^H + \boldsymbol{\phi}^H diag(\boldsymbol{f}_{RC}^H)\boldsymbol{F}_D)\boldsymbol{w}_D\right|^2 + \sigma_C^2} \,, \tag{14}$$

where $\boldsymbol{\phi} = [\phi_1, \phi_2, \ldots, \phi_N]^T$.

Denote $\boldsymbol{F}_{RC} = diag(\boldsymbol{f}_{RC}^H)\boldsymbol{F}_C$, $\bar{\boldsymbol{F}}_{RC} = diag(\boldsymbol{f}_{RC}^H)\boldsymbol{F}_D$, then (13a) can be written as

$$\frac{\left|(\boldsymbol{h}_C^H + \boldsymbol{\phi}^H \boldsymbol{F}_{RC})\boldsymbol{w}\right|^2}{\left|(\boldsymbol{h}_{DC}^H + \boldsymbol{\phi}^H \bar{\boldsymbol{F}}_{RC})\boldsymbol{w}_D\right|^2 + \sigma_C^2} \ge \gamma_1 \,. \tag{15}$$

The molecular moiety can be converted to as

$$\begin{aligned} \left|(\boldsymbol{h}_C^H + \boldsymbol{\phi}^H \boldsymbol{F}_{RC})\boldsymbol{w}\right|^2 &= \boldsymbol{w}^H(\boldsymbol{h}_C + \boldsymbol{F}_{RC}^H\boldsymbol{\phi})(\boldsymbol{h}_C^H + \boldsymbol{\phi}^H \boldsymbol{F}_{RC})\boldsymbol{w} \\ &= \boldsymbol{\phi}^H \boldsymbol{F}_{RC}\boldsymbol{w}\boldsymbol{w}^H\boldsymbol{F}_{RC}^H\boldsymbol{\phi} + 2\,\mathrm{Re}\left\{\boldsymbol{h}_C^H\boldsymbol{w}\boldsymbol{w}^H\boldsymbol{F}_{RC}^H\boldsymbol{\phi}\right\} + \boldsymbol{w}^H\boldsymbol{h}_C\boldsymbol{h}_C^H\boldsymbol{w} \end{aligned} . \tag{16}$$

Similarly, we have the following equations

$$\left|(\boldsymbol{h}_{DC}^H + \boldsymbol{\phi}^H \bar{\boldsymbol{F}}_{RC})\boldsymbol{w}_D\right|^2 = \boldsymbol{\phi}^H \bar{\boldsymbol{F}}_{RC}\boldsymbol{w}_D\boldsymbol{w}_D^H\bar{\boldsymbol{F}}_{RC}^H\boldsymbol{\phi} + 2\,\mathrm{Re}\left\{\boldsymbol{h}_{DC}^H\boldsymbol{w}_D\boldsymbol{w}_D^H\bar{\boldsymbol{F}}_{RC}^H\boldsymbol{\phi}\right\} + \boldsymbol{w}_D^H\boldsymbol{h}_{DC}\boldsymbol{h}_{DC}^H\boldsymbol{w}_D \,. \tag{17}$$

Substituting (16) and (17) into (15), we can obtain

$$\begin{aligned} &\boldsymbol{\phi}^H(\boldsymbol{F}_{RC}\boldsymbol{w}\boldsymbol{w}^H\boldsymbol{F}_{RC}^H - \gamma_1\bar{\boldsymbol{F}}_{RC}\boldsymbol{w}_D\boldsymbol{w}_D^H\bar{\boldsymbol{F}}_{RC}^H)\boldsymbol{\phi} + 2\,\mathrm{Re}\left\{(\boldsymbol{h}_C^H\boldsymbol{w}\boldsymbol{w}^H\boldsymbol{F}_{RC}^H - \gamma_1\boldsymbol{h}_{DC}^H\boldsymbol{w}_D\boldsymbol{w}_D^H\bar{\boldsymbol{F}}_{RC}^H)\boldsymbol{\phi}\right\} \\ &+(\boldsymbol{w}^H\boldsymbol{h}_C\boldsymbol{h}_C^H\boldsymbol{w} - \gamma_1\boldsymbol{w}_D^H\boldsymbol{h}_{DC}\boldsymbol{h}_{DC}^H\boldsymbol{w}_D) \ge \sigma_C^2\gamma_1 \end{aligned} . \tag{18}$$

Denote $\Omega_k = \boldsymbol{F}_{RC}\boldsymbol{w}\boldsymbol{w}^H\boldsymbol{F}_{RC}^H$, $\bar{\Omega}_k = \bar{\boldsymbol{F}}_{RC}\boldsymbol{w}_D\boldsymbol{w}_D^H\bar{\boldsymbol{F}}_{RC}^H$, $\boldsymbol{w}_k = \boldsymbol{h}_C^H\boldsymbol{w}\boldsymbol{w}^H\boldsymbol{F}_{RC}^H - \gamma_1\boldsymbol{h}_{DC}^H\boldsymbol{w}_D\boldsymbol{w}_D^H\bar{\boldsymbol{F}}_{RC}^H$, $\bar{\boldsymbol{w}}_k = \boldsymbol{w}^H\boldsymbol{h}_C\boldsymbol{h}_C^H\boldsymbol{w} - \gamma_1\boldsymbol{w}_D^H\boldsymbol{h}_{DC}\boldsymbol{h}_{DC}^H\boldsymbol{w}_D$, then we have

$$\boldsymbol{\phi}^H\Omega_k\boldsymbol{\phi} - \gamma_1\boldsymbol{\phi}^H\bar{\Omega}_k\boldsymbol{\phi} + 2\,\mathrm{Re}\left\{\boldsymbol{w}_k\boldsymbol{\phi}\right\} + \bar{\boldsymbol{w}}_k \ge \sigma_C^2\gamma_1 \,. \tag{19}$$

From the first-order Taylor expansion we get that $\boldsymbol{\phi}^H\Omega_k\boldsymbol{\phi}$ can be lower bounded by $2\,\mathrm{Re}\left\{\boldsymbol{\phi}^{(t)^H}\Omega_k\boldsymbol{\phi}\right\} - \boldsymbol{\phi}^{(t)^H}\Omega_k\boldsymbol{\phi}^{(t)}$, where $\boldsymbol{\phi}^{(t)}$ is the optimal solution at the t-th iteration. Substitute it into (19), we have

$$2\,\mathrm{Re}\{(\boldsymbol{\phi}^{(t)^H}\Omega_k + \boldsymbol{w}_k)\boldsymbol{\phi}\} - \boldsymbol{\phi}^{(t)^H}\Omega_k\boldsymbol{\phi}^{(t)} - \sigma_C^2\gamma_1 + \bar{\boldsymbol{w}}_k \ge \gamma_1\boldsymbol{\phi}^H\bar{\Omega}_k\boldsymbol{\phi} \,. \tag{20}$$

Thereby, constraint (13a) can be equivalently transformed into (20), which is a convex constraint.

Similarly, for constraint (13b), we have

$$\frac{\left|(\boldsymbol{h}_D^H+\boldsymbol{f}_{RD}^H\boldsymbol{\Phi}\boldsymbol{F}_D)\boldsymbol{w}_D\right|^2}{\left|(\boldsymbol{h}_{CD}^H+\boldsymbol{f}_{RD}^H\boldsymbol{\Phi}\boldsymbol{F}_C)\boldsymbol{w}\right|^2+\sigma_D^2}=\frac{\left|(\boldsymbol{h}_D^H+\boldsymbol{\phi}^H diag(\boldsymbol{f}_{RD}^H)\boldsymbol{F}_D)\boldsymbol{w}_D\right|^2}{\left|(\boldsymbol{h}_{CD}^H+\boldsymbol{\phi}^H diag(\boldsymbol{f}_{RD}^H)\boldsymbol{F}_C)\boldsymbol{w}\right|^2+\sigma_D^2}. \tag{21}$$

Denote $\boldsymbol{F}_{RD}=diag(\boldsymbol{f}_{RD}^H)\boldsymbol{F}_D$ and $\bar{\boldsymbol{F}}_{RD}=diag(\boldsymbol{f}_{RD}^H)\boldsymbol{F}_C$, constraint (13b) can be rewritten as

$$\frac{\left|(\boldsymbol{h}_D^H+\boldsymbol{\phi}^H\boldsymbol{F}_{RD})\boldsymbol{w}_D\right|^2}{\left|(\boldsymbol{h}_{CD}^H+\boldsymbol{\phi}^H\bar{\boldsymbol{F}}_{RD})\boldsymbol{w}\right|^2+\sigma_D^2}\ge\gamma_2. \tag{22}$$

The numerator and denominator are simplified as follows

$$\left|(\boldsymbol{h}_D^H+\boldsymbol{\phi}^H\boldsymbol{F}_{RD})\boldsymbol{w}_D\right|^2=\boldsymbol{\phi}^H\boldsymbol{F}_{RD}\boldsymbol{w}_D\boldsymbol{w}_D^H\boldsymbol{F}_{RD}^H\boldsymbol{\phi}+2\operatorname{Re}\left\{\boldsymbol{h}_D^H\boldsymbol{w}_D\boldsymbol{w}_D^H\boldsymbol{F}_{RD}^H\boldsymbol{\phi}\right\}+\boldsymbol{w}_D^H\boldsymbol{h}_D\boldsymbol{h}_D^H\boldsymbol{w}_D, \tag{23}$$

$$\left|(\boldsymbol{h}_{CD}^H+\boldsymbol{\phi}^H\bar{\boldsymbol{F}}_{RD})\boldsymbol{w}\right|^2=\boldsymbol{\phi}^H\bar{\boldsymbol{F}}_{RD}\boldsymbol{w}\boldsymbol{w}^H\bar{\boldsymbol{F}}_{RD}^H\boldsymbol{\phi}+2\operatorname{Re}\left\{\boldsymbol{h}_{CD}^H\boldsymbol{w}\boldsymbol{w}^H\bar{\boldsymbol{F}}_{RD}^H\boldsymbol{\phi}\right\}+\boldsymbol{w}^H\boldsymbol{h}_{CD}\boldsymbol{h}_{CD}^H\boldsymbol{w}. \tag{24}$$

Substituting (23) and (24) into (22), we have

$$\begin{gathered}\boldsymbol{\phi}^H(\boldsymbol{F}_{RD}\boldsymbol{w}_D\boldsymbol{w}_D^H\boldsymbol{F}_{RD}^H-\gamma_2\bar{\boldsymbol{F}}_{RD}\boldsymbol{w}\boldsymbol{w}^H\bar{\boldsymbol{F}}_{RD}^H)\boldsymbol{\phi}+2\operatorname{Re}\left\{(\boldsymbol{h}_D^H\boldsymbol{w}_D\boldsymbol{w}_D^H\boldsymbol{F}_{RD}^H-\gamma_2\boldsymbol{h}_{CD}^H\boldsymbol{w}\boldsymbol{w}^H\bar{\boldsymbol{F}}_{RD}^H)\boldsymbol{\phi}\right\}\\+(\boldsymbol{w}_D^H\boldsymbol{h}_D\boldsymbol{h}_D^H\boldsymbol{w}_D-\gamma_2\boldsymbol{w}^H\boldsymbol{h}_{CD}\boldsymbol{h}_{CD}^H\boldsymbol{w})\ge\sigma_D^2\gamma_2\end{gathered}. \tag{25}$$

Denote $\widehat{\Omega}_k=\boldsymbol{F}_{RD}\boldsymbol{w}_D\boldsymbol{w}_D^H\boldsymbol{F}_{RD}^H$, $\breve{\Omega}_k=\bar{\boldsymbol{F}}_{RD}\boldsymbol{w}\boldsymbol{w}^H\bar{\boldsymbol{F}}_{RD}^H$, $\widehat{\boldsymbol{w}}_k=\boldsymbol{h}_D^H\boldsymbol{w}_D\boldsymbol{w}_D^H\boldsymbol{F}_{RD}^H-\gamma_2\boldsymbol{h}_{CD}^H\boldsymbol{w}\boldsymbol{w}^H\bar{\boldsymbol{F}}_{RD}^H$, $\breve{\boldsymbol{w}}_k=\boldsymbol{w}_D^H\boldsymbol{h}_D\boldsymbol{h}_D^H\boldsymbol{w}_D-\gamma_2\boldsymbol{w}^H\boldsymbol{h}_{CD}\boldsymbol{h}_{CD}^H\boldsymbol{w}$. Inequality (25) be expressed as

$$\boldsymbol{\phi}^H\widehat{\Omega}_k\boldsymbol{\phi}-\gamma_2\boldsymbol{\phi}^H\breve{\Omega}_k\boldsymbol{\phi}+2\operatorname{Re}\left\{\widehat{\boldsymbol{w}}_k\boldsymbol{\phi}\right\}+\breve{\boldsymbol{w}}_k\ge\sigma_D^2\gamma_2. \tag{26}$$

From the first-order Taylor expansion we get that $\boldsymbol{\phi}^H\widehat{\Omega}_k\boldsymbol{\phi}$ can be lower bounded by $2\operatorname{Re}\left\{\boldsymbol{\phi}^{(t)^H}\widehat{\Omega}_k\boldsymbol{\phi}\right\}-\boldsymbol{\phi}^{(t)^H}\widehat{\Omega}_k\boldsymbol{\phi}^{(t)}$, where $\boldsymbol{\phi}^{(t)}$ is the optimal solution at the *t*-th iteration. Then, (26) can be transformed into

$$2\operatorname{Re}\{(\boldsymbol{\phi}^{(t)^H}\widehat{\Omega}_k+\widehat{\boldsymbol{w}}_k)\boldsymbol{\phi}\}-\boldsymbol{\phi}^{(t)^H}\widehat{\Omega}_k\boldsymbol{\phi}^{(t)}-\sigma_D^2\gamma_2+\breve{\boldsymbol{w}}_k\ge\gamma_2\boldsymbol{\phi}^{\boldsymbol{H}}\breve{\Omega}_k\boldsymbol{\phi}. \tag{27}$$

Hence, constraint (13b) can also be reformulated as a convex constraint.

To verify the feasibility of the problems, the constraint (20) and (27) can be further tightened by introducing slack variables $\boldsymbol{\varphi}=[\varphi_1,\varphi_2]$. Then, the expressions of (20) and (27) are

$$2\operatorname{Re}\left\{(\boldsymbol{\phi}^{(t)^H}\Omega_k+\boldsymbol{w}_k)\boldsymbol{\phi}\right\}-\boldsymbol{\phi}^{(t)^H}\Omega_k\boldsymbol{\phi}^{(t)}-\gamma_1\boldsymbol{\phi}^{\boldsymbol{H}}\bar{\Omega}_k\boldsymbol{\phi}+\bar{\boldsymbol{w}}_k\ge\sigma_C^2\gamma_1+\varphi_1, \tag{28}$$

$$2\operatorname{Re}\left\{(\boldsymbol{\phi}^{(t)^H}\widehat{\Omega}_k+\widehat{\boldsymbol{w}}_k)\boldsymbol{\phi}\right\}-\boldsymbol{\phi}^{(t)^H}\widehat{\Omega}_k\boldsymbol{\phi}^{(t)}-\gamma_2\boldsymbol{\phi}^{\boldsymbol{H}}\breve{\Omega}_k\boldsymbol{\phi}+\breve{\boldsymbol{w}}_k\ge\sigma_D^2\gamma_2+\varphi_2. \tag{29}$$

Constraint (13c) is non-convex, which can be modified into $1\le\left|\phi_n\right|^2\le1$ by the penalty CCP principle. Non-convex parts can be linearized with $\left|\phi_n^{(t)}\right|^2-2\operatorname{Re}(\phi_n^*\phi_n^{(t)})\le-1$. Finally, the optimization problem be constituted as P4.

$$\mathrm{P4}:\quad\max_{\boldsymbol{\varphi},\boldsymbol{\tau},\boldsymbol{\phi}}\sum_{\boldsymbol{k}=1}^{2}\varphi_k-\mu\sum_{\boldsymbol{n}=1}^{2\boldsymbol{N}}\tau_n, \tag{30}$$

$$s.t.\quad 2\operatorname{Re}\left\{(\boldsymbol{\phi}^{(t)^H}\Omega_k+\boldsymbol{w}_k)\boldsymbol{\phi}\right\}-\boldsymbol{\phi}^{(t)^H}\Omega_k\boldsymbol{\phi}^{(t)}-\gamma_1\boldsymbol{\phi}^{\boldsymbol{H}}\bar{\Omega}_k\boldsymbol{\phi}+\bar{\boldsymbol{w}}_k\ge\sigma_C^2\gamma_1+\varphi_1, \tag{30a}$$

$$2\operatorname{Re}\left\{(\boldsymbol{\phi}^{(t)^H}\widehat{\Omega}_k+\widehat{\boldsymbol{w}}_k)\boldsymbol{\phi}\right\}-\boldsymbol{\phi}^{(t)^H}\widehat{\Omega}_k\boldsymbol{\phi}^{(t)}-\gamma_2\boldsymbol{\phi}^{\boldsymbol{H}}\breve{\Omega}_k\boldsymbol{\phi}+\breve{\boldsymbol{w}}_k\ge\sigma_D^2\gamma_2+\varphi_2, \tag{30b}$$

$$\left|\phi_n^{(t)}\right|^2-2\operatorname{Re}(\phi_n^*\phi_n^{(t)})\le\tau_n-1,\forall n\in N, \tag{30c}$$

$$\left|\phi_n\right|^2\le1+\tau_{N+n},\forall n\in N, \tag{30d}$$

where $\boldsymbol{\tau}=[\tau_1,\tau_2,...,\tau_{2N}]^T$ is the slack variable and μ is the penalty factor. Problem P4 is a convex optimization problem which can be solved directly by CVX.

3.3 Overall algorithm and complexity analysis.

The proposed optimization algorithm can be summarized as Algorithm 1.

Algorithm 1: The Algorithm for Solving **P1**

Initialize $\boldsymbol{\phi}^{(0)}$ and $\boldsymbol{w}^{(0)}$, set $t=0$.
repeat
  Set $t_1=0$
  repeat
    With given $\boldsymbol{\phi}^{(t)}$ and $\boldsymbol{w}^{(t_1)}$, find the optimal $\boldsymbol{w}^{(t_1+1)}$ by solving **P2**.
    Set $t_1=t_1+1$.
  until the increment of the objective figure of **P2** is below a threshold $\epsilon>0$ or $t_1=T_{max}$.
  Set $t_2=0$, $\boldsymbol{w}^{(t)}=\boldsymbol{w}^{(t_1)}$ and $\boldsymbol{\phi}^{(t_2)}=\boldsymbol{\phi}^{(t)}$.
  repeat
    With given $\boldsymbol{w}^{(t)}$ and $\boldsymbol{\phi}^{(t_2)}$, find the optimal $\boldsymbol{\phi}^{(t_2+1)}$ by solving **P4.**
    Set $t_2=t_2+1$.
  until the increment of the objective figure of **P4** is below a threshold $\varepsilon>0$ or $t_2=T_{max}$.
  Set $t=t+1$, and $\boldsymbol{\phi}^{(t)}=\boldsymbol{\phi}^{(t_2)}$.
until the increment of the objective figure of **P1** is below a threshold $\varepsilon>0$ or $t=T_{max}$.

Complexity Analysis: The above proposed Algorithm 1 involves only the SOC constraint and the linear constraint. The linear constraint is not considered when calculating the complexity. We usually use equation (31) to calculate the complexity of the algorithm.

$$\mathcal{O}\left(\left(\sum_J J_j b_j + 2I\right)^{0.5} n\left(n^2 + n\sum_J J_j b_j^2 + \sum_J J_j b_j^3 + n\sum_I I_i a_i^2\right)\right), \tag{31}$$

In equation (31), I_i is the figure of SOC restrictions, which is of size a_i and has $\sum I_i = I$. J_j is the figure of LMI restrictions, which is of size b_j and $\sum J_j = J$. The parameter n represents the number of variables. For this paper, it is necessary to calculate the complexity of the problems P2 and P4, separately, and the overall complexity is the sum of them. According to (31), it is easily to obtain that $o_{\mathbf{w}}=\mathcal{O}\left(\sqrt{2}\,M_t^3\left(M_t+1\right)\right)$ and $o_{\boldsymbol{\Phi}}=\mathcal{O}\left(\sqrt{6}N^3\left(3N+1\right)\right)$ are the complexity of P2 and P4, respectively. Therefore, the overall complexity is $o=o_{\mathbf{w}}+o_{\boldsymbol{\Phi}}$.

4. Simulation Results

The performance and characteristic of the proposed method are provided in simulation results. The C-VUE vehicle and a pair of D-VUE vehicles are randomly generated according to the exponential distribution with a mean value of 2.5v, v is average vehicle speed. The BS and the IRS are deployed on both sides of the road. Taking the middle point on one side of the road as the coordinate origin, we set the coordinates of the BS as (0m, 0m, 20m) and the coordinates of the IRS as (0m, 12m, 20m). **Table 1** shows the parameters of the simulation[15].

Table 1. Simulation parameters

Parameter	value
The number of antennas of the BS M_t	3
The number of antennas of C-VUE M_r	1
The number of antennas of D-VUE1 L_t	3
The number of antennas of D-VUE2 L_r	1
Minimum transmit power of BS(dBm) P	30
Rice factor K	10
Penalty factor μ	10^{-5}
Minimum Received SINR of C-VUE(dB) γ_1	0.1
Minimum Received SINR of D-VUE2(dB) γ_2	0.1
The path loss exponents for BS-VUEs link	3.2
The path loss exponents for VUEs-VUEs link	3.2
The path loss exponents for BS-IRS link	2.2
The path loss exponents for IRS-VUEs link	2.2
The length of this road(m)	200
The width of this road(m)	12
Number of lanes	3
Average speed of the vehicles(km/h)	60
Antenna height of vehicle terminal(m)	1.5
Antenna heights for BS and IRS(m)	20
The ratio of reflector distance to wavelength d/λ	0.5

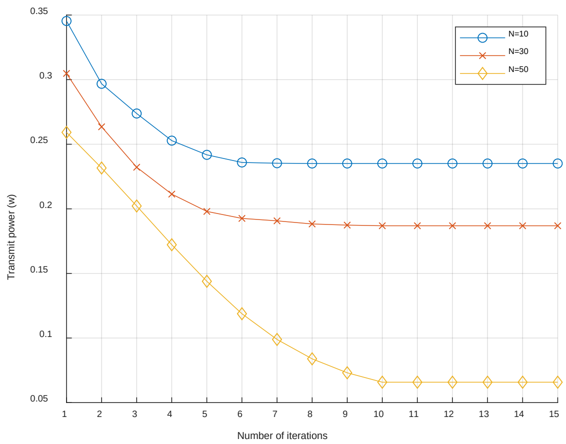

Fig. 2. Transmit power under different iterations

Fig. 2 indicates the alternate optimization algorithm proposed in this paper can converge within 10 iterations. N is set as 10, 30, and 50, which represents the number of phase shifts. **Fig. 2** shows that when the number of IRS phase shifts increases, the algorithm will converge to a smaller transmit power. Ultimate result shows the number of IRS phase shifts will affect the transmit power of the BS. Under certain constraints, the larger of N, the smaller of the required transmit power.

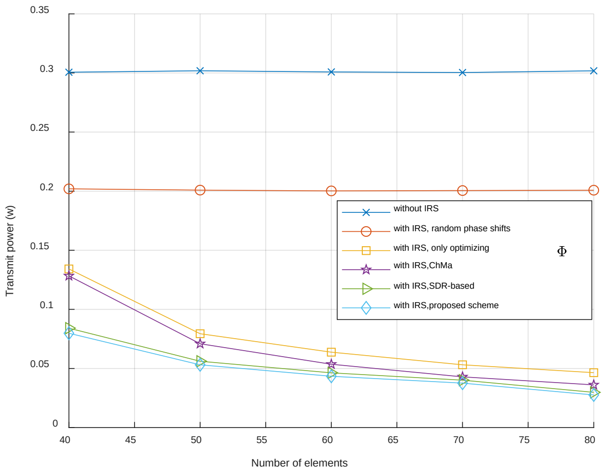

Fig. 3. The compare of different algorithms on the transmit power of the BS

In **Fig. 3**, we compare the proposed approach with several benchmark methods, benchmark methods include "without IRS", "with random phase shifts", "only optimizing $\mathbf{\Phi}$", "SDR-based", and "ChMa" algorithms. The algorithm "without IRS" means that the IRS is not used throughout the algorithm. The algorithm "with random phase shifts" means that the phases of the reflective elements are stochastically generated range in 0 and 2π. The algorithm "only optimizing $\mathbf{\Phi}$" means that the transmit precoding matrix is randomly generated and the phase shift matrix of the IRS is optimized by our proposed method. The algorithm "SDR-based" means that the optimization problem is solved by using semi-definite relaxation method. The algorithm "ChMa" is channel matching algorithm which means that the transmit precoding matrices $\boldsymbol{w}$ and $\boldsymbol{w}_D$ are both designed according to their SVDs of channels gain matrices, the phase shift matrix of the IRS is optimized by our proposed method. Fig. 3 shows that at the same number of IRS elements, the proposed optimization algorithm has the lowest BS transmit power. With the increase of the number of IRS elements, the transmit power decreases. Using SDR can also obtain low transmission power, however, according to [16], when using SDR to solve Pl, the Gaussian randomization process needs to be used to find the rank-one matrix solution, which results in an order of magnitude higher algorithm complexity with respect to the number of IRS elements compared with our proposed algorithm. Therefore, the deployment of IRS enables BS to achieve lower transmit power, thus verifies the superiority of the proposed method in this paper.

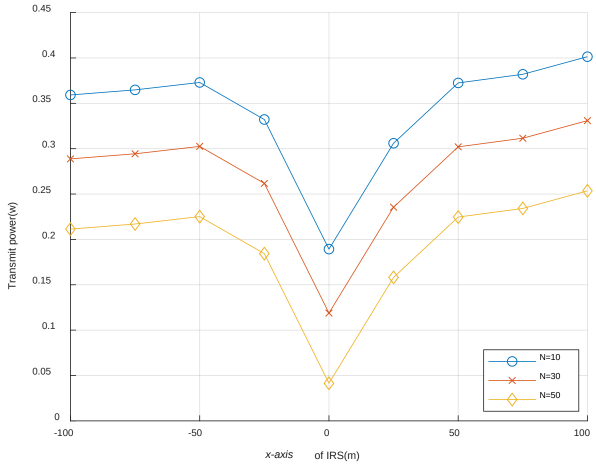

Fig. 4. Transmit power versus IRS location

Fig. 4 displays the relationship between the transmit power of the BS and the position of the IRS. In order to investigate the performance impact of the IRS on the minimum transmit power, the X-axis of the IRS is changed from -100m to 100m by moving the IRS along with the road side. When the X-axis of the IRS is 0, the IRS is closest to the BS. The phase shift numbers of the IRS are 10, 30 and 50, respectively. **Fig. 4** shows that when the X-axis of the IRS is 0, all of the three curves reach the lowest point, that is, when the IRS is deployed around the BS, the lowest transmit power can be achieved.

5. Conclusion

In this paper, by jointly designing the beamforming vector at BS and the phase shift matrix at IRS, the problem of minimizing the transmit power of the IRS-assisted vehicle communication is studied, where the V2I and V2V links share the same spectrum. In this paper, the beamforming vector and phase shift matrix of the original problem are optimized alternately, both the V2I and V2V requirements of SINR are guaranteed. The simulation results validate the effectiveness and advantages of our proposed joint beamforming design method in reducing the total transmit power of BS.

References

[1] J. Wang, K. Zhu and E. Hossain, "Green Internet of Vehicles (IoV) in the 6G Era: Toward Sustainable Vehicular Communications and Networking," *IEEE Transactions on Green Communications and Networking*, vol. 6, no. 1, pp. 391-423, March. 2022. Article (CrossRef Link)

[2] S. Wang and Y. Liao, "CSI intelligent feedback for massive MIMO systems in V2I scenarios," *China Communications*, vol. 18, no. 7, pp. 36-43, July. 2021. Article (CrossRef Link)

[3] Y. Lee, J. -H. Lee and Y. -C. Ko, "Beamforming Optimization for IRS-Assisted mmWave V2I Communication Systems via Reinforcement Learning," *IEEE Access*, vol. 10, pp. 60521-60533, 2022. Article (CrossRef Link)

[4] D. Dampahalage, K. B. Shashika Manosha, N. Rajatheva and M. Latva-aho, "Intelligent Reflecting Surface Aided Vehicular Communications," in *Proc. of 2020 IEEE Globecom Workshops (GC Workshops)*, pp. 1-6, 2020. Article (CrossRef Link)

[5] A. Al-Hilo, M. Samir, M. Elhattab, C. Assi and S. Sharafeddine, "Reconfigurable Intelligent Surface Enabled Vehicular Communication: Joint User Scheduling and Passive Beamforming," *IEEE Transactions on Vehicular Technology*, vol. 71, no. 3, pp. 2333-2345, March. 2022. Article (CrossRef Link)
[6] Salem, M. Rihan, L. Huang and A. M. Benaya, "Intelligent Reflecting Surface Assisted Hybrid Access Vehicular Communication: NOMA or OMA Contributes The Most," *IEEE Internet of Things Journal*, vol. 9, no. 19, pp. 18854-18866, 2022. Article (CrossRef Link)
[7] Pan et al., "Multicell MIMO Communications Relying on Intelligent Reflecting Surfaces," *IEEE Transactions on Wireless Communications*, vol. 19, no. 8, pp. 5218-5233, Aug. 2020. Article (CrossRef Link)
[8] Q. Wu and R. Zhang, "Intelligent Reflecting Surface Enhanced Wireless Network via Joint Active and Passive Beamforming," *IEEE Transactions on Wireless Communications*, vol. 18, no. 11, pp. 5394-5409, Nov. 2019. Article (CrossRef Link)
[9] Q. Wu and R. Zhang, "Towards Smart and Reconfigurable Environment: Intelligent Reflecting Surface Aided Wireless Network," *IEEE Communications Magazine*, vol. 58, no. 1, pp. 106-112, January. 2020. Article (CrossRef Link)
[10] Y. Yang, B. Zheng, S. Zhang and R. Zhang, "Intelligent Reflecting Surface Meets OFDM: Protocol Design and Rate Maximization," *IEEE Transactions on Communications*, vol. 68, no. 7, pp. 4522-4535, July. 2020. Article (CrossRef Link)
[11] L. Zhang, Y. Wang, W. Tao, Z. Jia, T. Song and C. Pan, "Intelligent Reflecting Surface Aided MIMO Cognitive Radio Systems," *IEEE Transactions on Vehicular Technology*, vol. 69, no. 10, pp. 11445-11457, Oct. 2020. Article (CrossRef Link)
[12] X. Guan, Q. Wu and R. Zhang, "Joint Power Control and Passive Beamforming in IRS-Assisted Spectrum Sharing," *IEEE Communications Letters*, vol. 24, no. 7, pp. 1553-1557, July. 2020. Article (CrossRef Link)
[13] Z. Sheng, A. Pressas, V. Ocheri, F. Ali, R. Rudd, and M. Nekovee, "Intelligent 5G vehicular networks: An integration of DSRC and mmWave communications," in *Proc. of 2018 International Conference on Information and Communication Technology Convergence (ICTC)*, pp. 571–576, 2018. Article (CrossRef Link)
[14] P. Wang, J. Fang, X. Yuan, Z. Chen and H. Li, "Intelligent Reflecting Surface-Assisted Millimeter Wave Communications: Joint Active and Passive Precoding Design," *IEEE Transactions on Vehicular Technology*, vol. 69, no. 12, pp. 14960-14973, Dec. 2020. Article (CrossRef Link)
[15] L. Zhang, C. Pan, Y. Wang, H. Ren and K. Wang, "Robust Beamforming Design for Intelligent Reflecting Surface Aided Cognitive Radio Systems With Imperfect Cascaded CSI," *IEEE Transactions on Cognitive Communications and Networking*, vol. 8, no. 1, pp. 186-201, March. 2022. Article (CrossRef Link)
[16] G. Zhou, C. Pan, H. Ren, K. Wang and Z. Peng, "Secure Wireless Communication in RIS-Aided MISO System With Hardware Impairments," *IEEE Wireless Communications Letters*, vol. 10, no. 6, pp. 1309-1313, June. 2021. Article (CrossRef Link)

Xiangping Kong studies at the School of Electrical and Information Engineering, Jiangsu University of Technology. Her research interest is active and passive beamforming design for Intelligent Reflecting Surface assisted vehicle communication.

Yu Wang (Member, IEEE) received the Ph.D degree in information and communication engineering from Southeast University, Nanjing, China, in 2018. Now she is currently an Associate Professor with the School of Electrical and Information Engineering, Jiangsu University of Technology, Changzhou, China. Her research interest is in the area of vehicular ad hoc networks, focusing on performance analysis. She has published several technical papers in journal such as IEEE TVT and conferences such as ICC and GLOBECOM.

Lei Zhang (Member, IEEE) received the Ph.D. degree in information and communication engineering from Southeast University, Nanjing, China, in 2016. He is currently an Associate Professor with the School of Electrical and Information Engineering, Jiangsu University of Technology, Changzhou, China. His research interests include cognitive radio, vehicular networks and intelligent reflecting surface.

Yulong Shang received his B.E. degree in communication engineering from PLA Information Engineering University, Zhengzhou, China, in 2010, and his M.E. degree and Ph.D. in electronic computer engineering from Chonnam National University, Gwangju, Korea in 2014 and 2018, respectively. Since 2018, he lectured at the School of Electrical and Information Engineering at Jiangsu University of Technology, Changzhou, China. His recent research interests include wireless communication, MIMO, digital broadcasting systems and deep learning.

Ziyan Jia received the B.E. degree from Nanjing University of Posts and Telecommunications, China in 2004, and the M.E. and Dr.Eng. degrees from Shinshu University, Japan in 2007 and 2010, respectively. Since 2011, he has been with Jiangsu University of Technology, China, first as a Lecturer and since 2013 as an Associate Professor. His current research interests include wireless sensor network, cellular networks, wireless ad hoc network, MIMO, OFDM, SC-FDMA, etc.